

Calculation of creepage discharge safety factors against the tangential component of electric fields in the insulation structure of power transformers

Arsalan HEKMATI*

Department of Electrical Engineering, Shahid Beheshti University, Tehran, Iran

Received: 19.04.2016

Accepted/Published Online: 27.12.2016

Final Version: 05.10.2017

Abstract: Creepage discharges are a main cause of insulation damage in power transformers during repeated tests or during operation. In this paper, a hazardous region in the insulation structure of power transformers (the interface between solid and liquid insulation at the top edge of a high-voltage electrode) is considered, and the impact of a very important factor of the surface discharge initiation and propagation (the tangential component of the electric field) on the strength of the insulation structure is investigated in power transformers. Insulation system reliability against this tangential component is presented as a safety factor. Two methods based on cumulative stress characteristics and breakdown probability are proposed for safety factor calculation and for the recognition of weak insulation regions. These methods provide essential information on insulation system design and optimization for reducing insulation deteriorations. A case study is performed on the insulation structure of a power transformer that failed during a test at the Iran Transfo Corporation. The redesigned transformer has shown no test failures in the past 10 years.

Key words: Insulation structure, power transformer, safety factor, creepage discharge

1. Introduction

The age of a power transformer is mainly the age of its insulation structure. Partial discharges have a serious impact on the progressive deterioration of the insulation system and may lead to ultimate failure [1]. The interface between the oil and paper insulation at the edge of high-voltage electrodes is one of the weakest regions of the insulation system in power transformers. The surface partial discharge in this interface is a very important phenomenon in power transformers because the inception voltage of partial discharge in the solid/liquid interface is lower than voltages resulting in partial discharge in both liquid and solid insulation separately [2–4]. Investigations have been performed on the initiation, propagation mechanisms, and characteristics of surface discharges in oil/paper interfaces [5–10]. The electrical stress on the liquid/solid interface contains tangential and normal components. The tangential component of the electric field, E_t , has a key role in the initiation and propagation of creepage discharge along the interface [2,11]. Cumulative stress characteristics, defined as the variation of the maximum average tangential electric field versus the length of partial paths inside a creepage path, have been proposed as a design criterion for the insulation structure of high-voltage components [2,12]. In this paper, a criterion is defined as the safety factor of the solid/liquid insulation materials and surfaces against the tangential and normal components of the electric field, which is applicable to the design process of the transformer insulation system. The spacing between the pressboard barriers in the transformer is determined by the strength of the intervening bulk oil gaps, which is dependent on

*Correspondence: a_hekmati@sbu.ac.ir

the normal component of the electric field. However, the safety factors regarding the tangential component of the electric field in the solid/liquid interfaces should be seriously considered in order to prevent the low strength of power transformers against creepage discharges, resulting in failure reports during tests or during operation. The breakdown process is quite time-dependent; therefore, it is affected by the way the voltage is applied. AC voltage, even at a lower amplitude, is more dangerous for an insulation structure than the impulse voltage [1]. Thus, in this paper, only a 1-min AC test is considered [13]. Although Siemens has limited the amplitude of the tangential electric field in the interface to 3 kV/mm in the AC test and 6.9 kV/mm in the lightning impulse test (Siemens Company Technical Document “TUB3: Insulation Design”), not only the E_t amplitude but also its distribution is important. For the studied transformer, the E_t amplitude is in this proposed range; however, its failure because of the surface discharge on the pressboard, which imposes high monetary losses for the manufacturer, obligated the Iran Transformer Research Institute (ITRI) to investigate causes and remedies. This paper proposes criteria for the assessment and measurement of the impact of the tangential electric field on the strength of the insulation structure in power transformers. The two proposed methods for calculation of safety factors against the tangential electric field rely on different empirical bases: using the cumulative stress method, which utilizes the average tangential electric fields on the partial paths inside a creepage path, and identifying the paths with the highest risk of surface discharge, by which the safety factor of the whole path is calculated. However, the breakdown probability method considers the failure probability of every element at a very small length along the creepage path and calculates both the failure probability and the safety factor of the creepage path with a direct formula. In this paper, the cumulative stress method has been extended to address the insulation safety factor for gaps with nonuniform electric fields that change direction along the gap. This type of study on real gaps has not yet been considered in the literature. Calculation of the insulation safety factors by the failure probability method is also proposed for the first time in this paper. The other contribution of this paper is the application of the proposed methods to the insulation structure of a real transformer under production with test failure reports and the comparison of two different approaches for the reliability evaluation of the insulation structure against creepage discharges. The consistency of the safety factor calculation results by the two methods with quite different theoretical bases provides verification for the proposed methods. After the evaluation of this particular transformer’s insulation system regarding surface discharge occurrence and identification of the weakest regions against creepage discharge, a redesign process starts calculating the tangential field safety factors with the proposed methods. The dimensions of the optimized design and the safety factor calculation results are presented. The fabricated transformer, under production now, has had no test failures in the past 10 years.

2. Safety factors of creepage paths with a uniform electric field

Experimental design criteria that present the insulation strength of the bulk oil gaps under uniform applied electric fields are extensively utilized in transformer insulation design. The oil gap strength versus the oil gap length is explained by Eq. (1) for a frequency of 60 Hz [2]:

$$E_0 = 16.86 \times d^{-0.37}, \quad (1)$$

where d is the oil gap length in millimeters and E_0 is the electrical strength of the oil gap in kV/mm. According to research by the Weidman Company [3,4], the insulation strength of the oil/paper interface against a uniform tangential electric field is approximately 70% of the oil strength, as shown in Eq. (2):

$$E_0 = 0.7 \times 16.86 \times d^{-0.37} = 11.80 \times d^{-0.37}, \quad (2)$$

where d is the length of the oil/paper interface in millimeters. These design criteria are usually plotted on a logarithmic scale, as in Figure 1, which shows the insulation strength of the oil/paper interface against uniform tangential electric fields in a 1-min AC test versus the length of this interface [3]. This criterion states that an interface of length d can withstand a uniform tangential electric field up to E_0 . Thus, in the case of a uniform tangential electric field of E , the safety factor of the creepage path along the interface may be simply defined as $SF = E_0/E$. However, for the nonuniform distribution of the electric field along an oil/paper interface, the safety factor cannot be calculated in the same manner. The impact of the electric field distribution on the reliability of the creepage path should therefore be investigated. According to [14], the oil strength under impulse voltage is almost 2.3 times the strength of the oil under 1-min AC voltage. Therefore, it is sufficient to regard the AC situation for safety factor calculation against the tangential electric field.

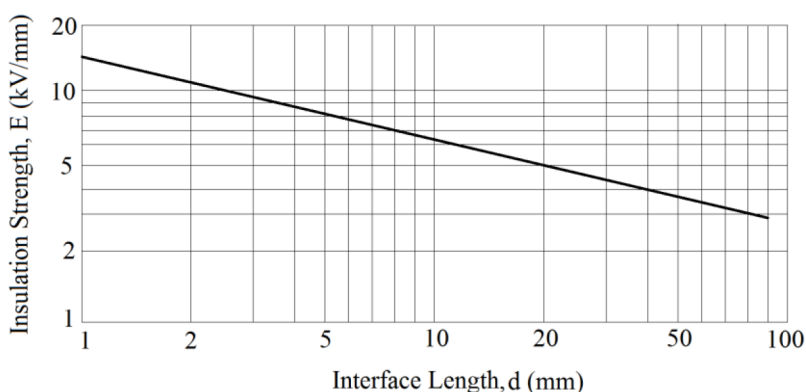


Figure 1. The insulation strength of the oil/paper interface versus its length [2].

3. Safety factors of creepage paths with a nonuniform electric field

Two methods have been utilized for the safety analysis of the creepage paths with nonuniform tangential electric fields.

3.1. The cumulative stress method

In order to investigate the safety of a creepage distance, any selected path of desired length from the total creepage distance (i.e. a partial path) should be checked against the creepage discharges. To accomplish this, the cumulative stress characteristic is used, and the average tangential electric field on any chosen partial path of any length is compared to the maximum value from Eq. (2). Almost all of the software for electric field analysis calculates the voltage or the electric field in discrete points on a creepage path, due to the numerical approaches for the solution of the related equations. Thus, the methodology for determination of safety margins for all partial paths in a creepage path should be based on discrete electric field data. In both the proposed methods in this paper, the cumulative stress method and the breakdown probability method, the gaps are divided into very small gaps where the electric field may be assumed to be constant with very good approximation. Apparently, by increasing the small gap lengths, the precision of these methods will decrease. It is evident that, considering all of the partial paths present in a long creepage distance and the great number of calculation points (for appropriate accuracy), it is a difficult and time-consuming process. Therefore, a method has been developed based on the cumulative stress characteristics [12] that identifies the partial paths of highest average electrical stress among all paths of same length and that calculates the safety factor for each path, while also providing the

overall safety factor of the creepage path. This method is based on the fact that the local maximum points of the electric field have the highest probability for partial discharge inception. Indeed, partial discharge is a local phenomenon, and all events are concentrated at high-stress points of the insulation structure [2,14] because one of the most important mechanisms of breakdown initiation is related to the charged particles' behavior. These particles can be swept to the highest stress point and cause a weak link (especially when moisture is present). Thus, high local stress is a prerequisite for partial discharge and failure initiation [2]. Therefore, the spans of the local maximum points have been chosen as the paths of the shortest length that have the greatest electrical stress among all paths of similar length. Other partial paths are acquired by expanding these paths by one step (the span of the calculated field points) from the endings in the direction that results in a greater average electric field. The safety factors of the partial paths are calculated at each step from $SF = E_0/E_{av}$, where E_{av} is the average electric field on the partial path and E_0 is calculated from Eq. (2) for the partial path length. The procedure is repeated until the entire creepage distance is covered. The safety factor of the whole creepage path is the minimum of the calculated safety factors and the partial path with the minimum safety factor, the critical partial path, is the weakest path on the creepage distance against the creepage discharge. At a point of zero stress on a surface, as there would be no creepage discharge initiating activity, the length scale on the cumulative stress curve should be reset [12]. In other words, regarding the field direction that is changed at the zero-crossing points of the electric field, continuing to average the electric field data along the creepage path would result in lower cumulative stress while seeking paths with maximum average electric field. Therefore, for the creepage paths with varying directions of tangential electric field, the safety factors are calculated for all the creepage paths between two adjacent zero-crossing points of the electric field and finally the safety factor of the whole creepage path will be the minimum of these calculated safety factors. The flowchart of the proposed cumulative stress method (averaging method) is shown in Figure 2.

3.2. The breakdown probability method

In this method, the creepage path is divided into units of very small length. The electric field would be approximately constant at each length element. According to the 'weakest link theory', the probability of an electrical breakdown is given with a Weibull distribution for a single unit, as shown in Eq. (3) [15,16]:

$$P_i = 1 - \exp \left\{ - \left(\frac{E_i}{E_{0i}} \right)^m \right\}, \quad (3)$$

where E_{0i} is the mean failure stress of the unit, E_i is the applied electric field to the path unit, and m is the constant shape parameter. The breakdown probability for the whole path consisting of n units would be as shown in Eq. (4):

$$P_{br} = 1 - \prod_i (1 - P_i) = 1 - \exp \left[- \sum_{i=1}^n \left(\frac{E_i}{E_{0i}} \right)^m \right]. \quad (4)$$

It may be shown, according to the Weibull distribution statistics, that if E_0 is the mean failure stress of unit volume or surface and n volumes or surfaces are tested together (yielding a mean failure stress of E_n), then $E_n = E_0/n^{\frac{1}{m}}$, in which n represents the oil volume or the creepage surface [2]. Thus, according to Eq. (2) and based on experimental experiences, the shape parameter of m would be $m = 1/0.37 = 2.7027$ and E_{0i} may be calculated according to the length of the unit path. To assign a safety factor to a creepage path, the relation between the failure probability and the safety factor should be investigated. The breakdown probability of a

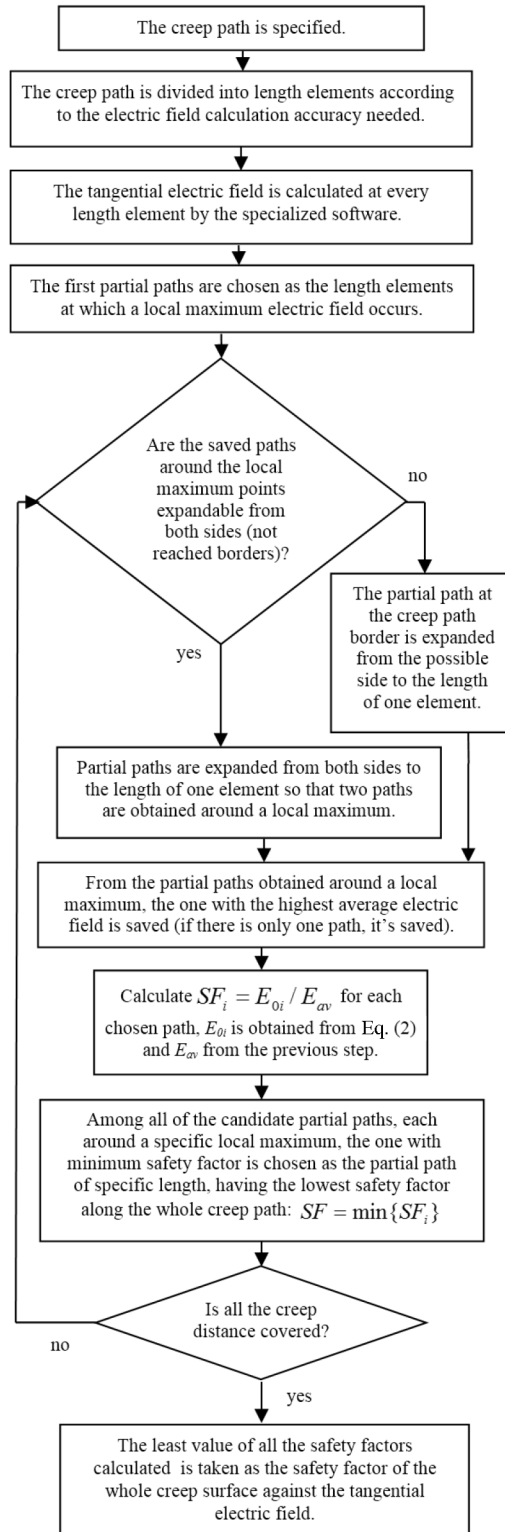


Figure 2. Flowchart of the cumulative stress method.

creepage path with a uniform electric field would be as presented in Eq. (5), according to Eq. (4):

$$P_{br} = 1 - \exp \left\{ - \left(\frac{E}{E_0} \right)^m \right\}, \quad (5)$$

where E_0 is the withstand electric field of the whole path from Eq. (2). As explained in Section 2, the safety factor of the path is $SF = \frac{E_0}{E}$; therefore, the relation between the breakdown probability and the safety factor would be as shown in Eq. (6):

$$P_{br} = 1 - \exp \left\{ - (SF)^{-m} \right\}. \quad (6)$$

Therefore, the safety factor may be expressed in terms of the breakdown probability, as seen in Eq. (7):

$$SF = (-\ln(1 - P_{br}))^{-\frac{1}{m}}. \quad (7)$$

The variation of creepage path safety factor versus its breakdown probability is plotted in Figure 3.

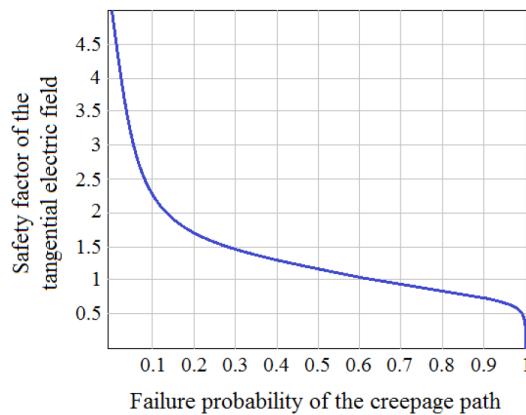


Figure 3. Variation of creepage path safety factor with breakdown probability.

According to Eqs. (4) and (7), the safety factor would be calculated as in Eq. (8):

$$SF = \left(\sum_{i=0}^n \left(\frac{E_i}{E_{0i}} \right)^m \right)^{-\frac{1}{m}}. \quad (8)$$

The two proposed algorithms are applied to a power transformer at the Iran Transfo Corporation, following several reports on an insulation failure at the top edge region of the HV electrode during a 1-min AC test for this transformer.

4. Case study

A 132/20-kV, 30-MVA power transformer of Siemens design has been modeled on the Axial Program (a program for Ax Symmetrical Electrostatic Field Calculation in Piecewise Homogenous Media, Iran Transformer Research Institute, ITRI, Version 1.1, 1997). Axial uses the finite difference method to solve the equations. In electrostatics, the governing equation is the Poisson equation in Eq. (9):

$$\nabla \cdot (\nabla V) = -\rho/\varepsilon, \quad (9)$$

where V is the electric potential, ρ is the charge density, and ε is the permittivity.

Because the windings and all of the other elements like the angle rings in every phase of the transformer have a rotational symmetry around the related core leg, as seen in Figure 4, where a 2D view of phase windings around a core leg are presented, the specialized Axial software independently analyzes each phase and solves Eq. (9) in a cylindrical coordinate system with rotational symmetry around the related core axis; therefore, it solves the 2D problem, as shown in Eq. (10):

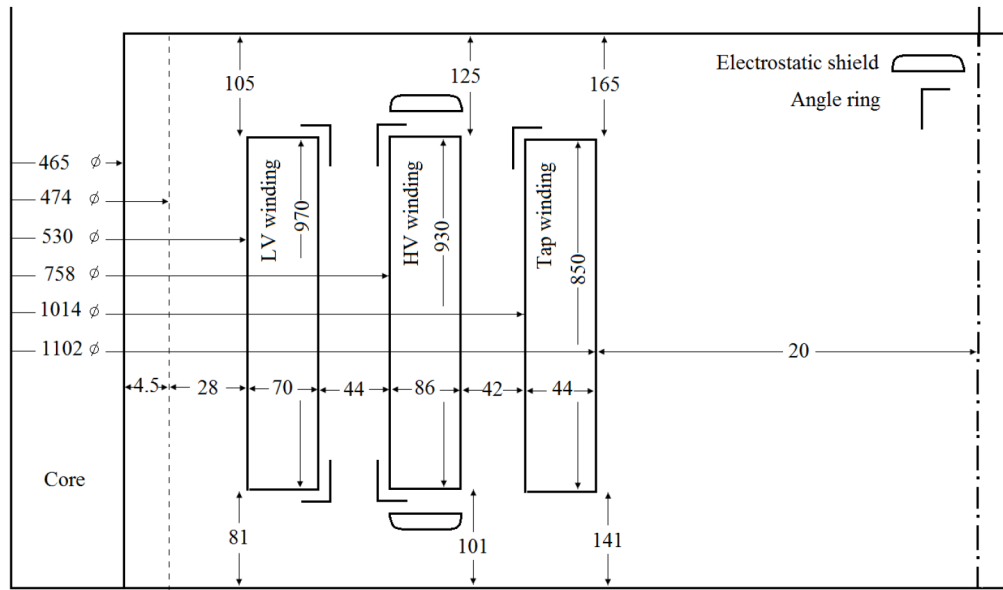


Figure 4. Dimensions of the transformer and the position of angle rings and static rings (all units in millimeters).

$$\frac{1}{r} \frac{\partial}{\partial r} \left(r \frac{\partial V}{\partial r} \right) + \frac{\partial^2 V}{\partial z^2} = 0. \quad (10)$$

The electric field is also calculated from $E = -\nabla V$.

Two boundary conditions are considered. At the interface between the two surfaces, Eq. (11) should be satisfied:

$$\hat{u} \cdot \Delta E = 0,$$

$$\hat{u} \cdot \Delta D = \rho_s, \quad (11)$$

where \hat{u} is the unit vector normal to the interface, ΔE is the change in electric field intensity (V/m), and ΔD is the change in electric flux density (C/m²).

At a perfectly conducting surface, Eq. (12) should be satisfied as the boundary condition:

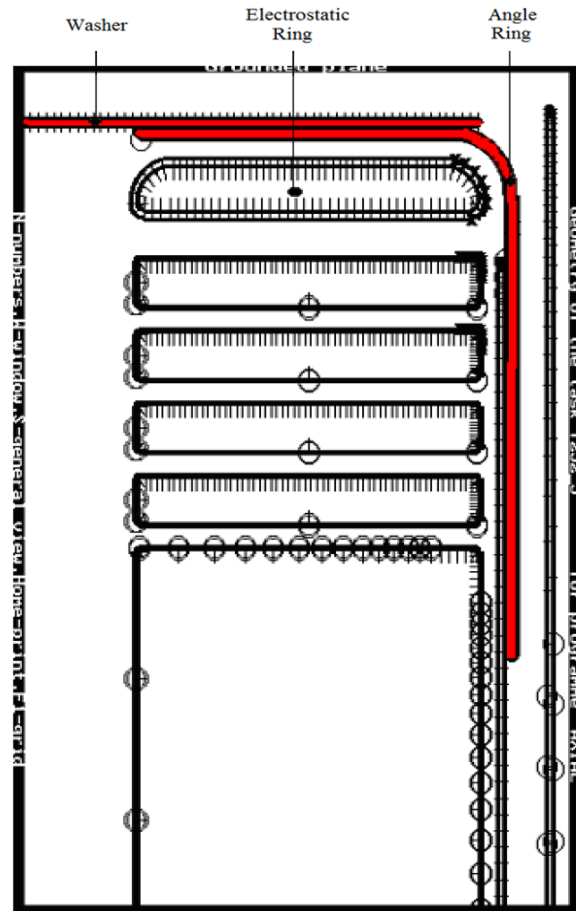
$$\hat{u} \times E = 0, \quad (12)$$

where \hat{u} is the unit vector normal to the interface pointing away from the conductor and E is the exterior electric field intensity (V/m). The material properties considered can be seen in Table 1.

Table 1. Material properties.

Copper conductivity	Relative permittivity of insulation paper	Relative permittivity of insulation pressboard	Relative permittivity of insulation oil
6×10^7 S/m	3.85	4.3	2.2

The studied transformer has nominal ratings, which are presented in Table 2. The HV and LV windings are disk-type and the two-tap windings (GROB and FEIN) are layer-type. The dimensions of the transformer and the position of angle rings and static rings are shown in Figure 4. This transformer has two static rings at the higher and lower edges of the HV electrode and five angle rings at the winding edges. All the angle rings and washers have a thickness of 3 mm. Figure 5 shows the simulation of the upper HV electrode edge and its insulation structure at the HV/LV gap. For the mesh generation, 22,000 triangular surface elements have been defined. The line-to-line voltage at the HV terminals of the studied transformer is 132 kV. According to Table 3, the HV winding is star connected (Y); therefore, the peak phase voltage for the HV electrode, considered the simulation boundary condition, is $132\sqrt{2}/\sqrt{3} = 107.78$ kV.

**Figure 5.** Insulation structure of the top edge of the HV electrode.

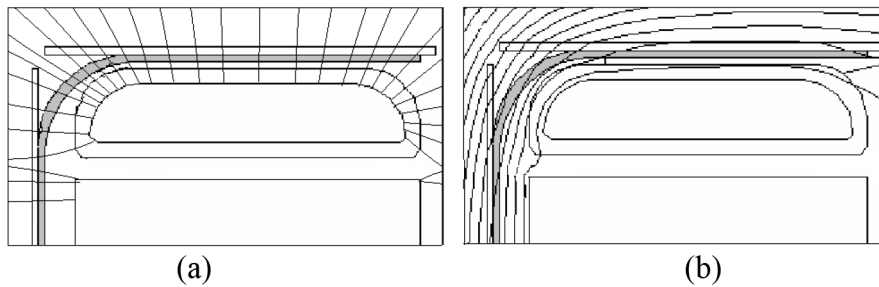
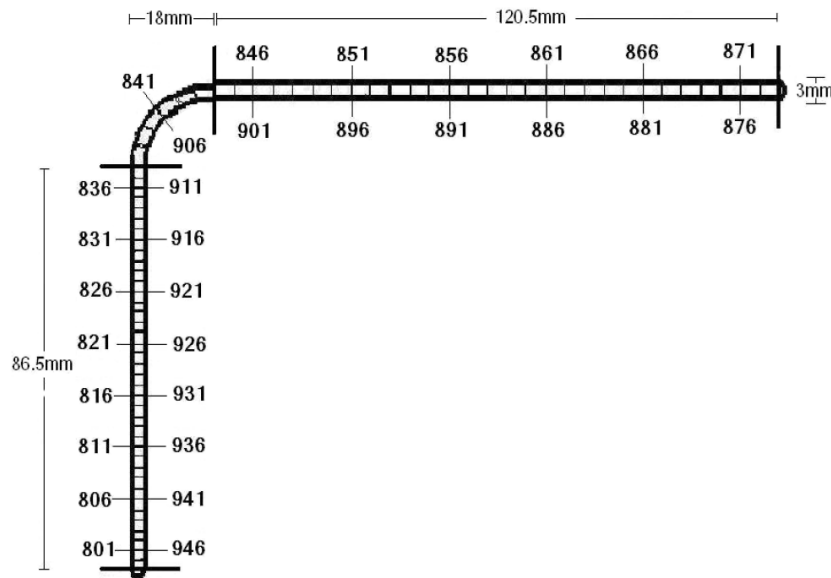
There are two pressboard insulators above the electrostatic ring at the top of the electrode: the angle ring and the washer upon the angle ring, as shown in Figure 5. To investigate the reliability of this insulation structure against the creepage discharge due to the tangential electric field, three creepage surfaces should be

Table 2. Nominal ratings of the 30-MVA, 132/20-kV transformer.

Cooling type	ONAF	Short circuit impedance	12.65%	Copper weight	6641 kg
HV connection	Yn	No load losses	26.5 kW	Core weight	1834 kg
LV connection	D	Full load losses	130 kW	Voltage tap	$\pm 15\%$

considered: 1) the angle ring surface in the top edge of the HV winding, 2) the surface of the washer upon the angle ring, and 3) the surface surrounding both elements.

The electric field and the equipotential lines at the top edge of the HV electrode are shown in Figure 6. The angle ring dimensions are shown in Figure 7. The angle ring has been divided into 150 elements in Axial (numbered from 799 to 948), and the value of the tangential electric field has been calculated at these points, as shown in Figure 8. These values are in percent per unit and with a base voltage of 230 kV in the induced voltage test (multiplying the per unit values by 2.3 yields the actual values of the tangential field in kV/mm). The flowchart in Figure 2 for the cumulative stress method has been implemented with MATLAB software and has been applied to the tangential electric field data, calculated by the Axial, for every path between two adjacent zero-crossings in the profile of Figure 8. Ten distinct paths on the surface of the angle ring are distinguished

**Figure 6.** a) The electric field lines and b) the equipotential lines.**Figure 7.** Dimensions of the angle ring at the top edge of the HV electrode.

and are shown in Figure 8. The safety factors should be calculated separately for every path. Dividing the creepage distance into several paths, each one between the two zero-crossing points of electric field, allows for consideration of the possibility of partial discharge initiation in all of the local maximum points. If the maximum average electric fields along the obtained partial paths are plotted logarithmically versus their length for each of the ten paths, the cumulative stress characteristic is obtained for that path, as seen in Figure 9. The nearest point to the insulation strength curve corresponds to the partial path with the minimum safety factor inside the path, as shown in Figure 9, and, as the critical partial path, its safety factor represents the safety factor of the whole creepage distance. The results of the safety factor calculation are presented in Table 3. The minimum calculated safety factor represents the safety factor of the angle ring surface, which is 2.97, according to Table 3. This safety factor belongs to the critical partial path with the electric field and position shown in Figures 10 and 11. The shown path is the weakest region on the angle ring from the viewpoint of creepage discharge initiation and propagation, and reinforcing this region would result in a lower possibility of partial discharge occurrences and a higher insulation strength of the angle ring. Similarly, the algorithm was applied

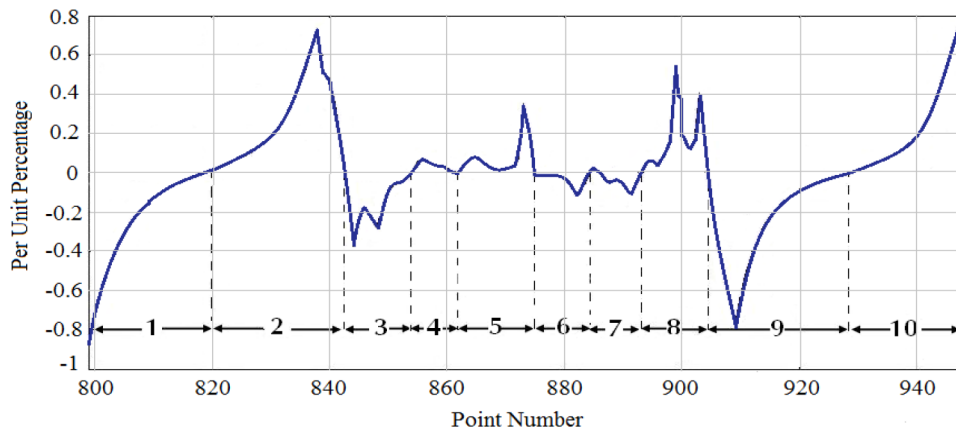


Figure 8. The tangential component of the electric field along the angle ring surface.

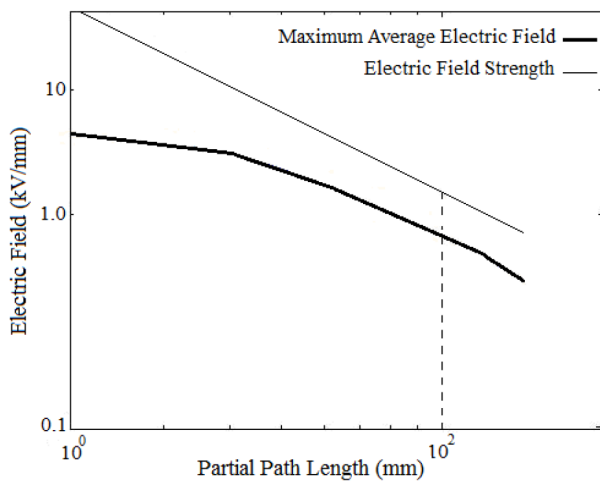


Figure 9. The insulation strength curve and the cumulative stress characteristic.

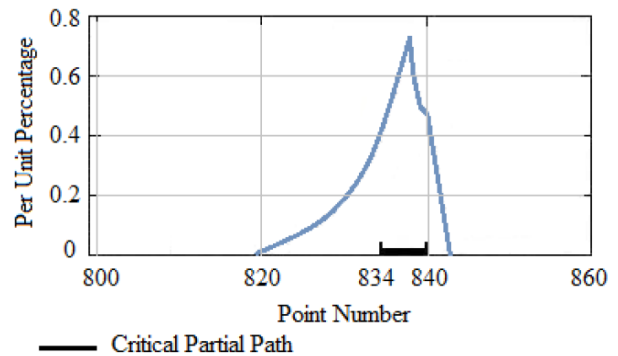


Figure 10. Position of the angle ring critical path on the tangential electric field profile (inside path number 2 in Figure 7).

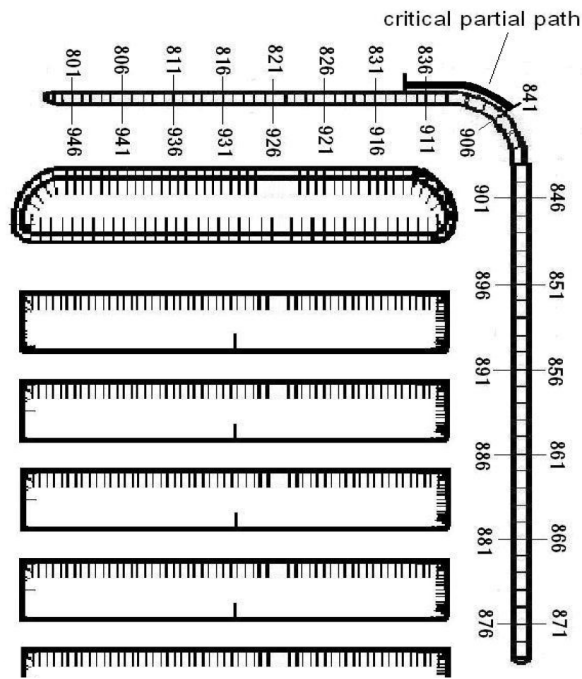


Figure 11. Position of the critical path on the angle ring.

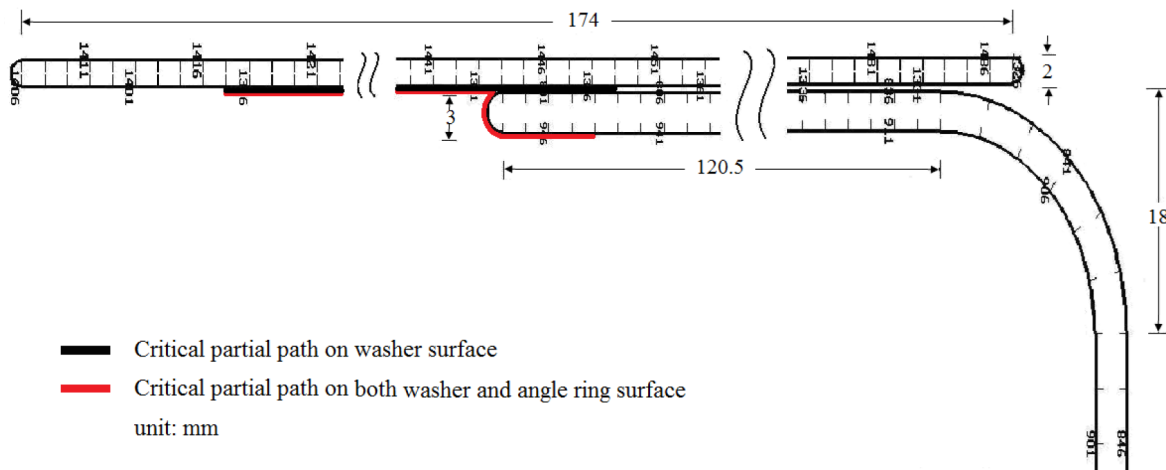


Figure 12. Partial path with minimum safety factor on washer surface on the angle ring.

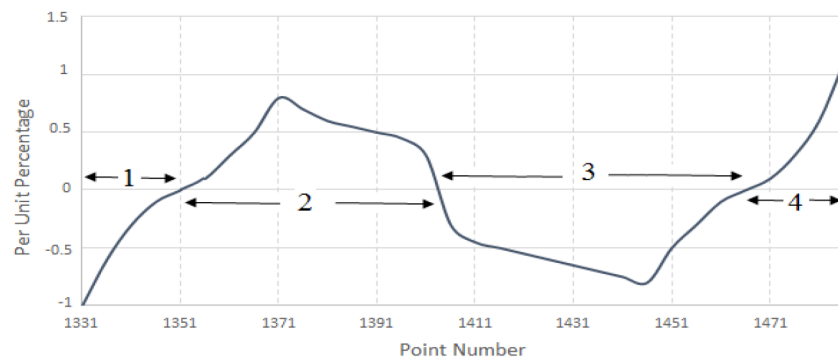


Figure 13. Tangential component of the electric field along the washer surface.

to the surface of the washer upon the angle ring, with dimensions as shown in Figure 12, and the tangential component of the electric field along the washer surface, as shown in Figure 13. The calculated safety factor is equal to 1.75 and is related to the critical partial path shown in Figure 12. Another path to be considered is the path around the two mentioned elements. The obtained safety factor is 1.73, with the critical partial path as shown in Figure 12. The washer has a lower safety factor because it is much wider than the angle ring; therefore, the washer surface has more electric field dispersion, which leads to longer partial paths with lower safety factors. In other words, there are lengthy partial paths on the washer, with a unidirectional tangential electric field, as shown in Figure 13, and these paths have lower insulation strengths. The failure probability method has also been applied to the three mentioned paths. The results are presented in Table 4. According to the electric potential distribution of the angle ring and washer surfaces of the transformer under the induced voltage withstand test (induced test) at 230 kV, the safety factors have been calculated for other electrode edges in a similar manner and the results are presented in Table 5. The insulation gaps and the angle ring and washer positions, thicknesses, and curvature radii have been varied in order to achieve a minimum safety factor of 2 in all of the considered gaps. For the new design, the thicknesses of the angle rings and washers are 5 mm and 4 mm for the upper edge of the HV/LV and HV/GROB gap, respectively. The thickness of the lower angle rings is unaltered. The curvature radii of the upper angle rings have been increased by approximately 30%. The new dimensions of the redesigned transformer are shown in Figure 14. The safety factors have been recalculated according to the proposed algorithm, and the results of Table 5 have been acquired. The fabricated transformer has not shown any failure since its fabrication in 2006.

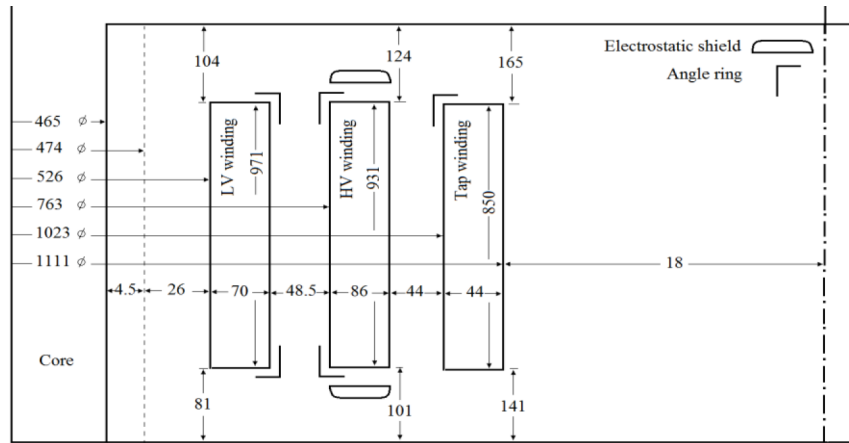


Figure 14. Dimensions of the redesigned transformer (all units in millimeters).

Table 3. Safety factors against the tangential electric field for the creepage paths on the angle ring.

Safety factor	Path number	Safety factor	Path number
34.3954	6	3.2860	1
24.4626	7	2.9726	2
5.5703	8	6.3868	3
3.1943	9	31.8563	4
3.2035	10	7.7117	5

Table 4. Comparison of safety factor calculation results with the two proposed methods.

Corresponding surface	Angle ring	Washer	Angle ring and washer
Failure probability method	2.93	1.74	1.71
Cumulative stress method	2.97	1.75	1.73

Table 5. Assessment of insulation structure safety factors for the old and redesigned transformer.

Gap	Old-upper edge	Redesigned upper edge	Old-lower edge	Redesigned lower edge
HV/LV	1.71	2.53	2.67	3.35
HV/GROB	1.06	2.00	2.75	3.57

5. Conclusion

In this paper, the impact of the tangential component of the electric field on the strength of the insulation structure against the creepage discharge in power transformers was evaluated. Methods to measure the safety factors of the tangential electric field were developed and applied to a sample power transformer. The calculation results from the two methods show good compatibility. Using these methods, recognizing the weak insulation regions from the viewpoint of the creepage discharge initiation and reinforcing them for more reliable transformer designs are possible. The failure probability method is simpler and easier to calculate; furthermore, it also yields the failure probability of the path, which sometimes provides better intuition than the safety factor. However, the cumulative stress method has the advantage of determining weak regions on the path related to creepage discharge propagation. The failure probability method may be extended to more complex surfaces of two or more materials or combinations of creepage surfaces and oil gaps, while the cumulative stress method applies only to homogeneous environments such as the creepage paths in oil/paper interfaces or in bulk oil gaps.

Regarding the calculated safety factors and determined critical partial paths in the case study, redesign and insulation structure improvements were performed for the studied transformer and no insulation failure reports have yet been received during different tests.

Acknowledgment

This work was supported by the Iran Transformer Research Institute and the Iran Transfo Company.

References

- [1] Hekmati A. Proposed method of partial discharge allocation with acoustic emission sensors within power transformers. *Appl Acoust* 2015; 100: 26-33.
- [2] Nelson JK. An assessment of the physical basis for the application of design criteria for dielectric structures. *IEEE T Electr Insul* 1989; 24: 835-847.
- [3] Tschudi DJ. AC Insulation Design: Paper-Oil Insulation Systems. In: *Proceedings of the WICOR Insulation Conference*; September 1996; Rapperswil, Switzerland. pp. 1-9.
- [4] Kim YH, Seok BY, Lee YJ, Koo JY. Experimental investigation of the effect of the design parameters of pressboard in mineral oil on creepage discharge propagation. *IET Sci Meas Technol* 2013; 7: 23-31.
- [5] Li J, Si W, Yao X, Li Y. Partial discharge characteristics over differently aged oil/pressboard interfaces. *IEEE T Dielect El In* 2009; 16: 1640-1647.
- [6] Liu Q, Wang ZD. Streamer characteristic and breakdown in synthetic and natural ester transformer liquids with pressboard interface under lightning impulse voltage. *IEEE T Dielect El In* 2011; 18: 1908-1917.

- [7] Yi X, Wang Z. Creepage discharge on pressboards in synthetic and natural ester transformer liquids under ac stress. *IET Electr Power App* 2013; 7: 191-198.
- [8] Saker A, Atten P. Properties of streamers in transformer oil. *IEEE T Dielect El In* 1996; 3: 784-791.
- [9] Okubo H, Okamura K, Ikeda M, Yanabu S. Creepage flashover characteristics of oil/pressboard interfaces and their scale effects. *IEEE T Power Deliver* 1987; 2: 126-132.
- [10] Nakao Y. Influence of insulating barrier on the creepage discharge in transformer oil. *IEEE T Dielect El In* 1997; 4: 775-779.
- [11] Moser HP. *Transformer Board*. 1st ed. Rapperswil, Switzerland: Scientia Electrica; 1979.
- [12] Nelson JK. Some steps toward the automation of the design of composite dielectric structures. *IEEE T Dielect El In* 1994; 1: 663-671.
- [13] IEC. *IEC Standard 60076-3. Power Transformers-Part 3: Insulation Levels, Dielectric Tests and External Clearances in Air*. 2nd ed. Geneva, Switzerland: IEC Publications; 2000.
- [14] Siodla K, Ziomek W, Kuffel E. The volume and area effect in transformer oil. In: *International Symposium on Electrical Insulation*; 7–10 April 2002; Boston, MA, USA. New York, NY, USA: IEEE. pp. 359-362.
- [15] Kurita H, Hasegawa T, Kimura K. Dielectric breakdown characteristics of clean oil. In: *International Symposium on Electrical Insulation*; 7–10 June 1992; Baltimore, MD, USA. New York, NY, USA: IEEE. pp. 433-436.
- [16] Gerhold J, Hubman M, Telsner E. Breakdown probability and size effect in liquid helium. *IEEE T Dielect El In* 1998; 5: 321-333.